Landslide susceptibility modelling using integrated application of computational intelligence in Ahar County, Iran

Solmaz Abdollahizad[1], Mohammad Ali Balafar[2*], Bakhtiar Feizizadeh[3], Amin Babazadeh Sangar[4], Karim Samadzamini[5]
Department of IT and Computer Engineering, Urmia Branch, Islamic Azad University, Urmia, Iran[1,2,3,4]
Department. IT. Faculty of Electrical and Computer Engineering. University of Tabriz[2]
Department of Remote sensing and GIS, University of Tabriz, Tabriz, Iran[3]
Department of Computer Engineering, University College of Nabi Akram, Tabriz, Iran[5]
Email: balafarila@yahoo.com

Abstract

Landslide susceptibility analysis is beneficial information for a wide range of applications. We aimed to explore and compare three machine learning (ML) techniques, namely the random forests (RF), support vector machine (SVM) and multiple layer neural networks (MLP) for landslide susceptibility assessment in the Ahar county of Iran. To achieve this goal, 10 landslide occurrence-related influencing factors were pondered. A sum of 266 locations with landslide potentiality was recognized in the context of the study, and the Pearson correlation technique utilized in order to select the influencing factors in landslide models. The association between landslides and conditioning factors was also evaluated using a probability certainty factor (PCF) model. Three landslide models (SVM, RF, and MLP) were structured by the training dataset. Lastly, the receiver operating characteristic (ROC) and statistical procedures were employed to validate and contrast the predictive capability of the obtained three models. The findings of the study in terms of the Pearson correlation technique method for the importance ranking of conditioning factors in the context area uncovered that slope, aspect, normalized difference vegetation index (NDVI), and elevation have the highest impact on the occurrence of the landslide. All in all, the MLP model had the utmost rate of prediction capability (85.22 %), after which, the SVM model (78.26 %) and the RF model (75.22 %) demonstrated the second and third rates. Besides, the study revealed that benefiting the optimal machine with the proper selection of the techniques could facilitate landslide susceptibility modeling.

Keywords: Random Forest, Support Vector Machine, Multiple Layer Neural Network

1. Introduction

Landslides are complex natural disasters that are frequently initiated several fatalities and casualties globally[1]. These occurrences have the potential to risk the lives of people and infrastructures of the nations in various areas around the world with immense social-economic consequences [2]. To this end, pinpointing the zones with landslide vulnerability is an effective technique to avert and decrease plausible damages. The landslide susceptibility modeling is extensively acknowledged that prediction accuracy outcomes are highly relies on the exploited data quality, conditioning factors, environmental conditions, topographic features of the region, and landslide inventory. Therefore, landslide susceptibility mapping (LSM) is multi-criteria in nature which requires several indicators from different resources to be taken into account of spatial modeling [3].

A review of research background signifies that various methods of preparing hazard maps and landslide susceptibility have recently been established using statistics, deterministic, and heuristic Statistical models, such as multivariate analysis [4], weights of evidence [5], Probabilistic models (e.g., FR) [6] evidential belief function [7], analytical hierarchy process [8], and Certainty factor [9] have been exploited by a great deal of the aforementioned studies. The heuristic method is developed in accordance with experts-related ideas and experiences with the intention of assigning various weights to different influencing factors. Nevertheless,

the method would not produce satisfactory results due to the limited study area data and low rate of reproducibility [6]. The deterministic model entails in-depth features of slopes [10] and is not appropriate for landslide susceptibility appraisals owing to the potential complications in the modeling and calculation procedure [11].

The involvement of judgments with subjectivity as well as disability in the quantification of each contributing factor is among the main shortcomings of the so-called qualitative or semi-quantitative approaches. The outcomes of these approaches are sensitive to the exports' knowledge, which makes them subjective to some extent. Quantitative methods exploit the mathematically-induced models in order to measure the landslide occurrence plausibility in an area and specify the hazardous zone on a continuous scale [12]. Studies that are conducted on landslide susceptibility have also used machine learning (ML) in their modellings due to the enhanced processing capability of the ML on the data in dynamic conditions or environments with uncertainty. For instance, models such as Naive Bayes [13],[14], Multi-Layer Perceptron [15],[16], Decision Tree [17], Neuro-Fuzzy [18], Support Vector Machine [19], Logistic Regression [20], and Reduced Error Pruning Trees [21] are among the so-called ML methods. Therefore, ML approaches are considered to be promising in spatial prediction of landslide.

Although plenty of methods and models have been exploited to create maps of landslide susceptibility by geographic information systems (GIS), there is not a compromised method to be accepted as the most appropriate one due to the possible limitations of the qualitative techniques caused by unplanned occurrences or inadequate knowledge upon which the expert decisions are centered on. Conversely, inaccuracy, and imprecision of data are among the shortfalls of quantitative methods [22]. As indicated, due to a number of methods and techniques, recognizing and identifying the most efficient methods and techniques are still challenging. Based on this statement, the present study, it was of interest to investigate the efficiency of all the contributing factors in the assessments of landslide susceptibility and to contrast landslide susceptibility models on the basis of SVM, RF, and MLP in East Azerbaijan, Iran.

2. Study area and dataset

The study area was set to be in Ahar county at East Azerbaijan province (EAP) located northwest of Iran. This area is an important state in terms of housing, and human settlement. This area is also critical for the economy of the country by hosting a high number of industrial and agricultural activities [23],[24]. The geological and geotechnical structure and setting of EAP make this area highly susceptible to natural hazards such as earthquakes, mass movement, and landslides [25],[26]. Landslides are a typical phenomenon in EAP and earthquakes, volcanic threats, and landslides are caused by the lithological units-related complexities of the geological structure, which encompassed various formations [27],[28],[29].

A total number of 26 known landslide events are listed as a landslide inventory database in this region [30]. The area has sophisticated geology and the lithological units include numerous formations, which cause earthquakes, volcanic threats, and landslides. The geophysical characteristics of the area developed slops with extensive vulnerability to landslides mass movements (e.g., flows, creeps, rockfall, topples, and landslides) [30],[31]. [30], field observations statements, and lithological units reported that a great deal of landslide events could be reckoned to be of rotational landslides (Figure 1).

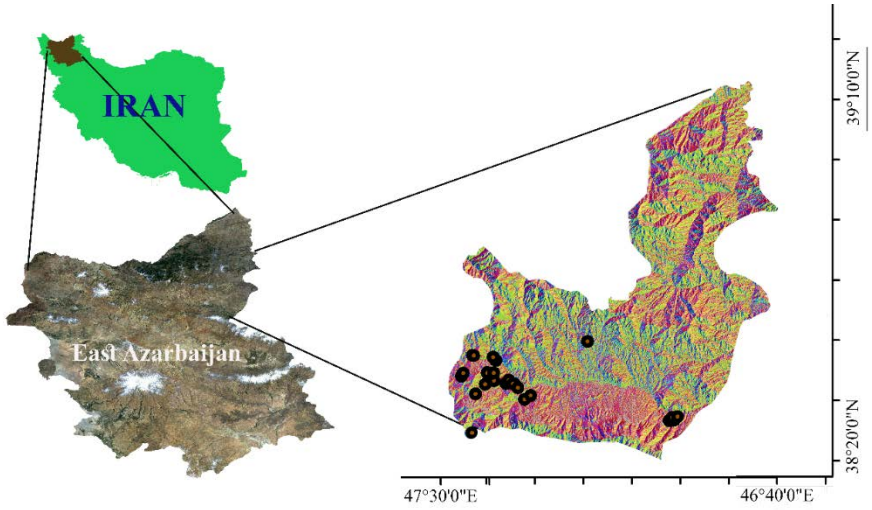

Fig. 1. Research area

3. Material and Methods

The assessment process was divided into four steps: The first step was establishing the spatial database. The second phase was choosing the conditioning factors and data correlation analysis. The third step was considered to generate the landslide susceptibility-related maps. Finally, the last stage was set to compare and validate the three ML methods using MLP, SVM, and RF models (Figure 2).

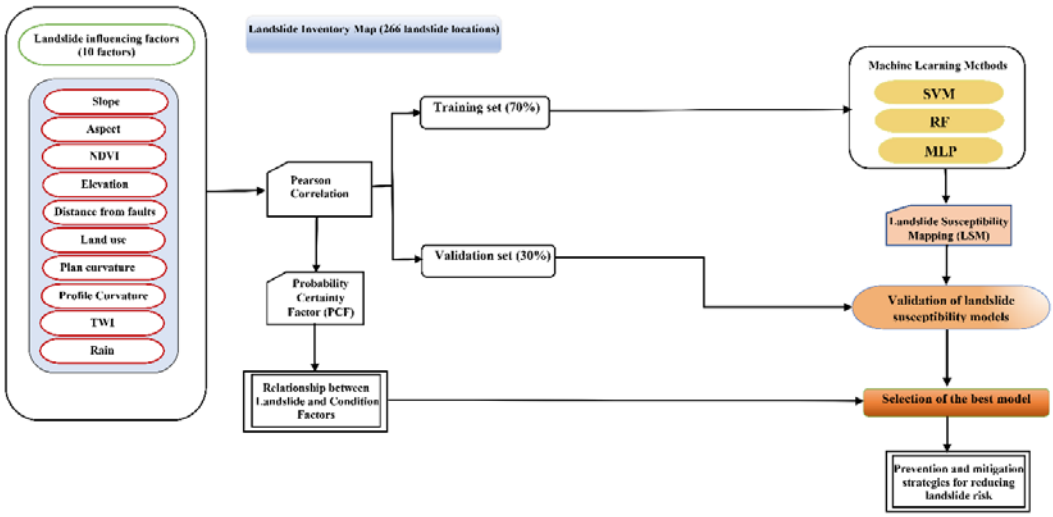

Fig. 2. Flowchart of the study

3.1 Preparation of data

3.1.1 Landslide inventory map

A crucial input for scrutinizing the correlation between the locations' spatial distribution and conditioning factors is the landslide inventory map [32]. Hence, in the present study, a landslide inventory map was prepared via historical data on individual landslide occurrences, all-embracing field surveys corroborated by the Iran National Cartographic Center and Geological Organization also with handheld GPS devices, interpretation of aerial photographs and Google Earth images.

A sum of 266 landslides was finally mapped in the study (Figure 3) and comprehensive reports on landslides have been exploited within a lifespan of > 37 years (since 1983). The landslides with the

smallest and largest sizes found in the study were nearly 200 and 3000 (m^2) respectively. For landslide spatial modelling through the so-called amalgamation of models, the locations of the landslide were separated into two subdivisions (viz., training (70) and validating (30) appertaining to a random selection scheme [33]. Figure 4 indicates a series of recorded landslides in the field surveys[34].

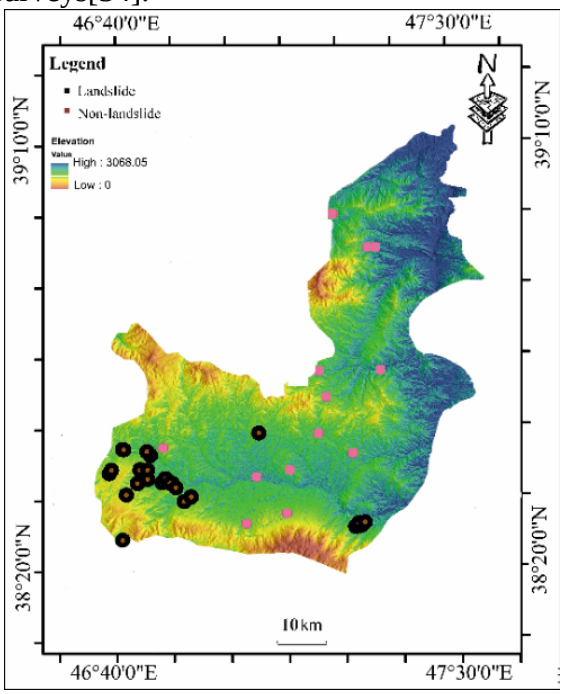

Fig.3. Landslide events map at study area

Fig.4. A photograph of landslides in the field survey

3.1.2 Preparation of Dataset for spatial modelling

Along with the landslide inventory map, numerous inter-related factors impact the landslides [35]. A total of 10 landslide influencing factors,

including slope, aspect, NDVI, elevation, distance from fault, land use, plan curvature, profile curvature, TWI, and rain were used in the proposed framework for spatial modeling [36].

In the present study, the ESRI ArcGIS 10.3 software was utilized with the intention of producing and displaying the data layers. All the layers of data were organized in raster format with a pixel size of 30 (m)×30 (m). The influencing factors were obtained from ASTER Global DEM , the geological map, and a topographic map with the same resolution [37]. Then the geological map was used in order to obtain the lithology map, which was then converted into a raster format. Landsat 8 (OLI images) were used in order to derive the NDVI as well as land use maps. For further analyses, all the so-called factors were standardized by a similar scale of 30 ×30 (m^2). Besides, the conditioning factors that were of continuous data were reclassified into distinct subsections with the intention of transforming continuous data to sections at specific intervals. In order to achieve the identical output scaling, the other discrete conditioning variables were reclassified into groups (Figure 5). For training/modelling, 186 (70%) landslide locations were utilized in the present analysis, and 80 (30%) landslides were utilized for validating. A value of "1" was allocated to the landslide training instances [38]. Moreover, from the landslide-free zones, a similar amount of non-landslide points (266) was randomly produced, and a value of '0' was allocated to these instances, which were randomly divided into two sections with a ratio of 70/30 as well

.

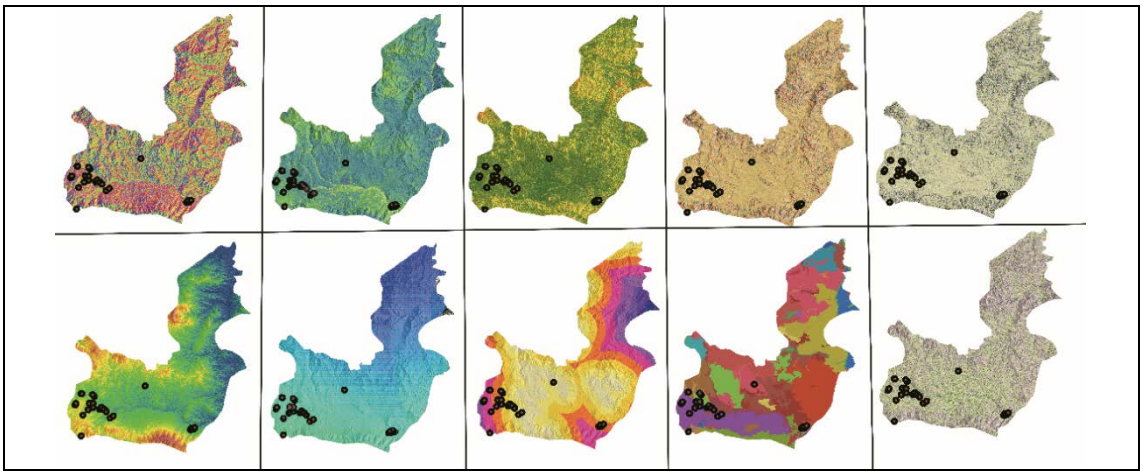

Figure 5. Ten condition factors map

3.1.3 Data correlation analysis

The PCF approach was employed in the present analysis to disclose the relationship between landslides and conditioning factors. Numerous researchers have used the so-called approach for landslide susceptibility mapping due to its suitability at dealing with ambiguity in the input data [39]. The PCF can be determined using the equation below:

$$PCF = \begin{cases} \dfrac{PP_c - PP_s}{PP_C(1 - pp_s)}, & PP_c \geq PP_s \\ \dfrac{PP_c - PP_s}{PP_s(1 - PP_c)}, & PP_c < PP_s \end{cases} \qquad (1)$$

where PP_c denotes the conditional probability of a landslide in category c, and PP_s is the preceding probability of landslides' total number in the current research regions. The certainty variables vary from −1 to 1, with −1 denoting certainly false and 1 denoting certainly true. A positive value indicates growing confidence in the occurrence of a landslide, whereas a negative value indicates that the occurrence likelihood of a landslide is declining, and a value near to 0 indicates that it is challenging to deliver data regarding the landslide occurrence certainty[40].

3.2 Landslide susceptibility modeling

3.2.1 RF

RF is regarded as an ensemble learning method that classifies unidentified samples predicated on the combined outcomes of a series of weak classifications Trees developed via bootstrapping techniques [41]. Particularly, the learning process includes choosing the predictor variable for each iteration and resampling the data through replacement [42]. By means of this approach, an RF model demonstrates a higher efficient ability to prevent overfitting problems and by and large present a superior generalization output [19].

In a randomized forest, the best split amid a subcategory of predictors, which are haphazardly selected by the node is used to split each node. Inherently, inside huge datasets, it has been a prominent technique for identifying beneficial hitherto invisible patterns. There are n variables that could be selected as random subsections from the training data with the intention of determining the best possible node to split. The best node division could be finalized utilizing Gini criteria [43]. The so-called criteria gauge the degree of association between variables and results.

The smallest value is regarded to be the optimal split for every node in accordance with the RF algorithm [44]. The Gini criteria are expressed as:

$$\mathrm{Gini}(k, x_i) = \sum_{i=1}^{m} \frac{a_i}{n_s} I(k_{ui}) \qquad (2)$$

Where the number of landslides is represented by m at each node *k*, and n_s is the indicator of training input function vectors. The class labels distribution at every node is

represented by $I(k_{ui})$. The p-value of node k is a feature variable $x_i \in X$ where $x_i = \{u_1, u_2, \ldots u_m\}$ and the $I(k_{ui})$ value could be calculated as:

$$I(k_{ui}) = 1 - \sum_{i=0}^{c} \frac{n_{ci}^2}{a_i^2} \quad (3)$$

where n_{ci} are the c_i-fitting samples with u_i values and ai denotes the number of samples that have the *ui* value at node *k*.

Through the training data and the n-fold cross-validation (n=10), the RF model was also developed. The num Iteration's parameter, which is the number of iterations to be executed, was differed to obtain the RF model's most optimum output. A heuristic test was performed, and once num Iterations were 1400, the AUC had the largest value. Afterwards, the subsequent RF model was utilized with the intention of calculating the values of LSI for the entire research area. These values vary between 0 and 1 and were re-categorized into five grades.

3.2.2 SWM

SVM is a series of techniques for ML on the basis of the notion of an optimum hyperplane of separation. In feature space, SVM considers the widest margin between the two groups. As it could be observed in Fig. 5, a standard SVM model could be of a two-class or multi-class model (an amalgamation of a two-class SVMs chain). The most widely used form of ML is the two-class SVM [38]. The separating hyperplane is among the possible planes, which divides two groups during the model performance. In Figure 6(a), the squares and dots reflect two sample groups, L being the in-between classification line, and L1 and L2 being lines running parallel to L across the sample points nearest to the classification line. The classification margin is considered to be the distance between them. The purpose of the optimum hyperplane classification is to correctly distinguish (although some errors are permitted) between the two types of samples while maximizing the support vector margin. Figure 6(b) shows the function of the kernel that aids to map the input samples into high-dimension space such that they could be linearly categorized [45]. In general, there are two categories of SVMs on the basis of object classification, viz. the two-class and multiclass. The multiclass SVM is a synthesis of a set of two-class SVMs [46]. Presently, pairwise classification and the one-to-the-other-class approach are prevalent multi-class SVM methods [47]. The most commonly used technique is two-class SVM. Normally, along with grouping, SVM could be exploited for regression analysis [48]. The results in the current analysis indicated that the sigma values and support vectors' number in the SVM model were 142 and 0.068, respectively. In addition, 0.118 and -91.5624 were calculated as the training error values and objective function, respectively.

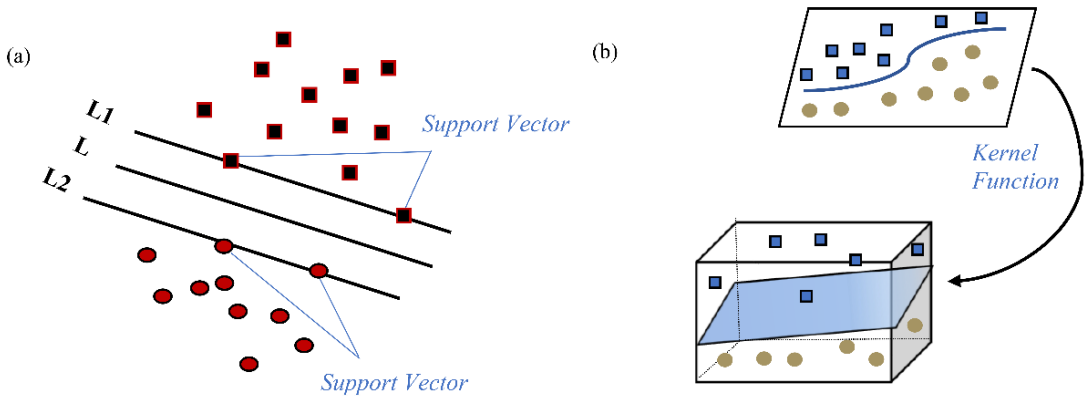

Fig.6. Classification of SVM (a) support line (b) hyperplane

3.2.2 Artificial Neural Network

Artificial neural networks (ANN) are units for the processing of computational information influenced by the behavior and structure of actual biological neurons whose architecture attempts to mimic the human brain cells' acquisition of knowledge and organizational skills. A benefit of ANNs is that some of the previously unknown hidden information could be utilized in the data. The benefits contain the fact that within an entire data set, they identify various data sets, they do not need any pre-existing experience or knowledge, and they do not require a pre-existing statistical model for training the data[49].The MLP was implemented in the current analysis. The most prevalent and frequently used ANN architecture is MLP, which is consisted of an output layer, an input layer, and in between hidden layers. In a network, each layer includes an adequate number of neurons. The output layer generates the outcomes of the neural network. Hence, the neurons' number in the layers is determined by the problem for which the network was developed. The inputs are processed by every output and hidden neuron layer through multiplying each input (x_i) with a respective weight (w_i), summating the product (Eq. (6)), and thenceforth processing the total (the neuron is subsequently activated if that surpasses the threshold of the neuron) by a non-linear activation function (Eq. (7)) to generate the output node result (y_i).

$$net = \sum_{i=0}^{n} w_i x_i \quad (4)$$

$$y_i = f(net) \quad (5)$$

A three-layer feed-forward ANN has been constructed. Following trial and error and cogitating the lowest error, the optimal network architecture was chosen. Initial weights in a limited range were initiated by random. Once the stopping error criteria are met, the process is terminated. The first objective in this analysis was to fulfill the stopping criteria of the root mean square error (RMSE). If RMSE is not attained, the epochs number could then be used as a termination criterion, which was set to be 1000 in the current analysis [16].The learning rate and momentum training parameters were considered to be 0.4 and 0.3, respectively. The network training activation transition function was considered to be hyperbolic tangent for the whole layers. Figure. 7 demonstrates the architecture of a multi-layered neural network. For every cell through n neurons, the landslide susceptibility is then estimated in the hidden layers as:

$$LS = f\left(\sum_{i=1}^{n} w_{ir}\, f\left(\sum_{j=1}^{m} v_{rj}\, u_j + b_r\right) + c_y\right) \quad (6)$$

Where adjusted weights are w_{ir} and v_{rj}, uj and y signify m×1 vector layer of input and output, b_r and c_y are biases of neuron in the output layer and hidden layers.

3.3 Model performance evaluation

The validity of the exploited models must be checked in the landslide susceptibility investigation since, without validation, they have little empirical value [50]. The ROC curve, which plots the rate of sensitivity on the y-axis in contrast to 1-specificity on the x-axis, has been utilized with the intention of validating the models in the present analysis. In order to have a comparison of three models, the AUC could be utilized. The values of 0 and 1 in AUC denotes a non-informative and a perfect model respectively [51]; and values could be labelled as bad, decent, good, very good, and exceptional once they fit in the range of (0.5-0.6), (0.6-0.7), (0.7-0.8), (0.8-0.9), and (0.9-1), respectively [52]. In Table 1, the so-called statistical measures were determined via the related formulas[53].

Table 1 Statistical indexes used in evaluation

Item	Description
MSE	$MSE = \frac{1}{n}\sum_{i=1}^{n}(T_i - O_i)^2$
RMSE	$RMSE = \sqrt{\frac{1}{n}\sum_{i=1}^{n}(T_i - O_i)^2}$
AUC	$AUC = \frac{(\sum TP + \sum TN)}{(P + N)}$

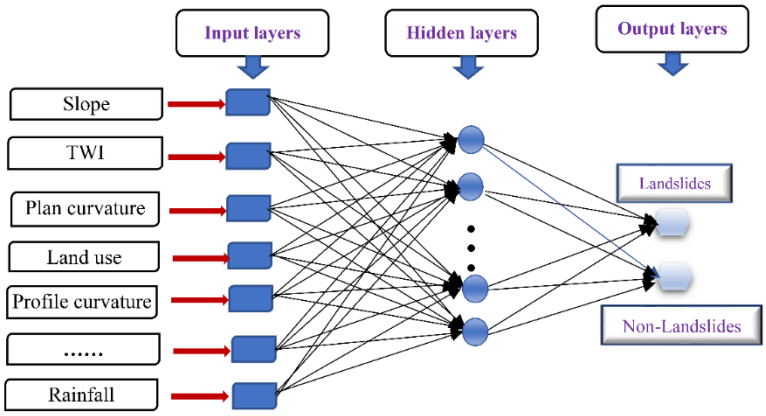

Fig.7. The layers of MLP

where P and N are the sum of the landslide and non-landslide numbers. The number of pixels that are correctly categorized are TP and TN (true positive and true negative). FP and FN (false positive and false negative) are the number of pixels that are wrongly classified [38]. A higher value implies a superior model for the AUC and a value with 1 index is an indicator of a perfect model [54].

4. Results

4.1 Analysis of conditioning factors

It is critical to choose appropriate variables for landslide modeling in landslide susceptibility assessment since conditioning factors in the training dataset might not be self-regulating of one another, which could initiate confusing noise into the model [55]. As a result, the conditioning factor's predictive capabilities ought to be measured, and elements with predictiveness of low or null must be eliminated. In order to calculate the predictive power of ten influential elements in the present study, the Pearson correlation test [56] was employed. The Pearson test was chosen for its capability in feature assortment in data mining [57]. With the increase in efficacy of the influencing variables in the model, the mean of Pearson correlation value and its SD increase correspondingly. The average and its standard deviation values are calculated from the Pearson correlation values by a 10-fold cross-validation technique (Table 2).

In correlations to the landslide in the sample region, there was a strong distinction in the predictive powers of ten influencing variables. The slope factor has the maximum AM value of 0.417 among these variables, indicating its significance compared to the others. Between 0.313 and 0.083 are the AM values for aspect, NDVI, TWI, distance from fault, elevation, land use, profile curvature, rain, plan curvature, and slope length. None of the factors is omitted in the study due to their predictive potential for the landslide.

Table 2. Landslide factors prediction power of using the Pearson correlation

factors	Average predictive power	Standard deviation
Slope	0.417	±0.016
Aspect	0.313	±0.015
NDVI	0.295	±0.017
Elevation	0.270	±0.013
Distance from fault	0.169	±0.015
Use Land	0.123	±0.007
Plan curvature	0.113	±0.002
Profile curvature	0.101	±0.002
TWI	0.087	±0.003
Rain	0.083	±0.002

Table 3 also shows the spatial association between landslides and influencing variables utilizing the PCF model. In line with the measured data, the PCF value for the slope angle class of >40° (0.742) is the highest, indicating the uppermost likelihood of landslide occurrence. The findings indicate that the slopes facing southeast (0.662) and south (0.533) have the maximum PCF values. The maximum PCF value of 0.447 is found between 1300 and 1600 m(elevation). Flat regions have the minimum PCF value, while the class of convex holds the maximum PCF value of 0.080 in terms of plan curvature. The maximum PCF value for TWI is contained in groups of >7. The class of >13000 m represents the greatest risk of a landslide occurrence with the distance to the faults (0.717). The flat profile curvature has the maximum PCF value, while the convex profile curvature holds the lowest PCF value. In the case of NDVI, the PCF value for the 0.05–0.15 range is the largest (0.502). As it comes to rainfall, the class of >310 mm holds the strongest relationship with the occurrence of landslides (0.682). Once it comes to land use, category B4 holds the maximum PCF value of 0.368, indicating the maximum likelihood of a landslide.

Table 3 Influencing factors and landslides relationship by PCF method

Factors	Sub-classes	Number of landslides	Landslide ratio (%)	Domain ratio (%)	PCF
1-Elevation	<1300	9	3.4	19.2	-0.224
	1300-1600	34	12.8	14.3	0.447
	1600-1900	110	41.3	28.9	0.373
	1900-2200	45	16.9	17.4	0.303
	>2200	68	25.6	20.2	0.260
2-Slope	<10	41	15.4	27.8	0.103
	10-20	86	32.3	29.8	0.507
	20-30	63	23.7	22.3	0.471
	30-40	41	15.4	11.7	0.496
	>40	35	13.2	8.4	0.742
3-NDVI	<0.05	13	4.9	27.1	-0.198
	0.05-0.15	131	49.2	24.9	0.502
	0.15-0.25	105	39.4	30.1	0.467
	>0.25	17	6.4	17.9	-0.236
4-Aspect	Flat	9	3.4	24.8	0.084
	North	17	6.4	9.7	0.226
	Northeast	59	22.1	10.4	0.412
	East	28	10.5	14.5	0.398
	Southeast	64	24.1	10.1	0.662
	South	28	10.5	13.7	0.533
	Southwest	13	4.9	9.5	0.178
	West	14	4.9	5.8	0.218
	Northwest	34	12.8	1.5	0.461
5-Distance from fault	<4000	31	11.6	34.7	0.170
	4000-7000	69	25.9	30.9	0.248
	7000-10000	5	1.9	7.5	0.104
	10000-13000	41	15.4	12.2	0.496
	>13000	120	45.1	14.7	0.717
6-Landuse	B2	8	3.0	9.7	0.240
	B3	9	3.4	12.6	0.177
	B4	249	93.6	77.7	0.368
7-Plan curvature	<-2	7	2.6	22.3	-0.170
	-2-0	128	48.1	36.7	-0.462
	0-2	113	42.9	32.4	-0.081
	>2	18	6.8	8.6	0.080
8-Profile curvature	<-2	14	5.3	31.2	-0.162
	-2-0	109	40.9	35.6	0.268
	0-2	124	4.7	22.9	0.715
	>2	19	7.1	10.3	0.138
9-TWI	<1	43	16.1	20.4	0.107
	1-3	116	43.6	39.1	0.216
	3-5	63	23.7	24.7	0.445
	5-7	25	9.4	9.7	0.481

	>7	19	7.1	6.1	0.659
10-Rain	<280	98	36.8	25.8	0.507
	280-290	64	24.1	28.4	0.450
	290-300	21	7.9	15.2	0.157
	300-310	23	8.6	24.5	-0.131
	>310	60	22.5	6.1	0.682

4.2 Validation and comparison of ML models

4.2.1 Model results and analysis

The training dataset was exploited to develop MLP Neural Nets, SVM, and RF through the fittest conditioning factors, the result of which could be observed in Tables 4 and 5. Regarding classification AUC and precision, it can be unearthed that the MLP models have the best efficiency. It is followed by the SVM and the RF models. The Kappa index ranged from 0.601 to 0.718 for the three models, which suggests a considerable compromise between the models and the actual situation.

The uppermost positive predictive value (PPV) belongs to the MLP model (94.96%) which shows the likelihood of the correct classification of the pixels by the model in 94.96% of the cases in the landslide class. It is followed by the SVM model (78.17 %), and the RF model (76.31 %). Nonetheless, the MLP model demonstrated the minimum negative predictive value (NPV) (75.93 percent), which suggests that the likelihood of pixels' correctly classification to the non-landslide class is merely 75.93%. The SVM (84.14%) model has the maximum value, which is followed by the RF (81.90%) along with the MLP Neural Networks. The highest sensitivity belongs to the SVM model (83.13%), which suggests that 83.13% of the landslide pixels are appropriately categorized into the landslide class that is followed by the RF model (80.83%) and the MLP model (79.78%). The highest specificity belongs to the MLP Neural Nets model (93.78%), which suggests that 93.78% of the non-landslide pixels are categorized correctly, which is followed by the SVM (79.40 %) and the RF (77.56 %).
The MLP, SVM, and RF were utilized to measure the landslide susceptibility indices for the whole pixels available in the study context once they were efficaciously trained in the testing stage. Landslide susceptibility indices have been reclassified into five classes of susceptibility through the area classification method.

Table 4. The performance of ML Models

Item	RF	MLP	SVM
PPV (%)	79.91	97.09	81.21
NPV (%)	83.73	77.17	86.02
Sensitivity (%)	82.08	82.10	84.96
Specificity (%)	79.11	94.81	80.83
Accuracy (%)	81.33	86.96	83.41
AUC	0.891	0.960	0.924
Kappa index	0.681	0.744	0.679

Table 5. Evaluation of three ML models on training data

Item	RF	MLP	SVM
PPV(%)	79.03	94.40	80.76
NPV (%)	83.67	78.09	84.72
Sensitivity (%)	84.20	80.14	83.05
Specificity (%)	78.96	85.48	80.70
Accuracy (%)	81.12	83.14	81.96
AUC	0.880	0.936	0.892
Kappa index	0.647	0.720	0.639

4.2.2 Model validation

Through the validation dataset, the Kappa index, the ROC curve, and the statistical assessment stages, the prediction likelihood of the susceptibility models was evaluated. Tables 6 and 7 demonstrate the results. It could be observed that for the MLP model (AUC=0.907), all of the models demonstrated a strong prediction capacity for the maximum one. The Kappa index ranged from 0.627 to 0.631, which indicates a robust compromise between the observed landslides and predicted ones (Table 6).

While the MLP model (85.22%) demonstrated the maximum likelihood of pixels' correct classification to the landslide class, the RF and SVM models are most likely to correctly assign pixels to the non-landslide classes (Table 7). For the RF model, sensitivity possessed the highest degree (85.02%), indicating that 85.02% of landslide pixels are accurately labeled as landslides. The MLP model displays the maximum specificity value (83.96%), which indicates that 85.38% of non-landslide pixels are appropriately grouped into the non-landslide class.

In Figure 8, the final maps of susceptibility are depicted. The indices were reclassified through the natural breaks method [58],[59] into five categories (i.e., very high, high, moderate, low, and very low) with the intention of enhancing the visualization. the validation of the susceptibility maps was carried out by contrasting them to the currently available landslide data.

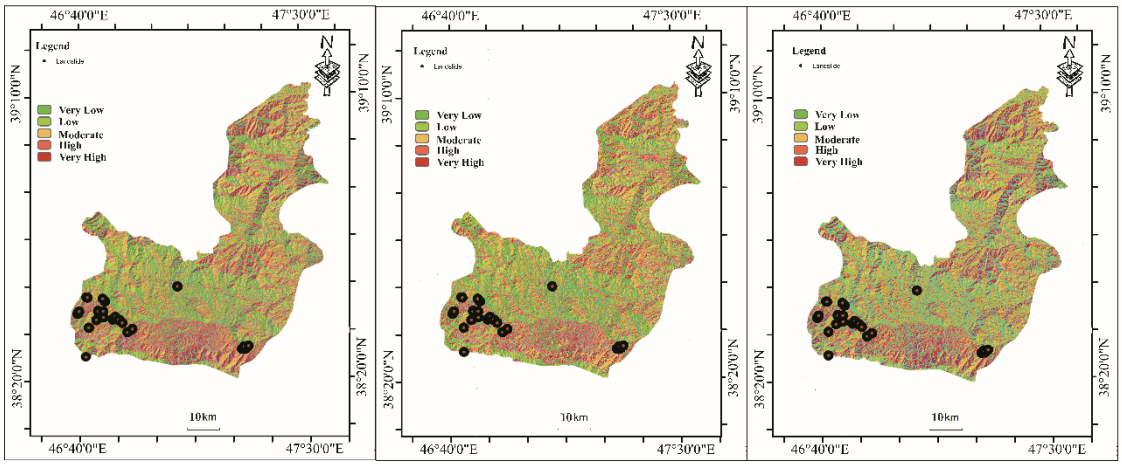

Fig.8. LSM using a) RF b) MLP c) SVM

The AUC reflects the model's strength percentage. The 0.9 to 1.0 variance is the optimal condition. The entire cells of 100 LSI values subsections in the study region and landslide incidents' cumulative percentage in the all classes determined the AUC. Elevated accuracies of susceptibility have been achieved using the so-called ML methods. For the MLP neural networks, SVM and RF methods, the relevant AUC values of 0.907, 0.883, and 0.869 were attained, which demonstrate that the map, which is derived through the MLP, indicated a higher accuracy than the one produced out of the SVM and RF outcomes.

On the basis of training and validation results, Figure 9 indicates the landslide pixels' ratio (%) for every susceptibility class to the sum of landslide pixels for maps of landslide sustainability (obtained by the methods of SVM, RF, and MLP, respectively).

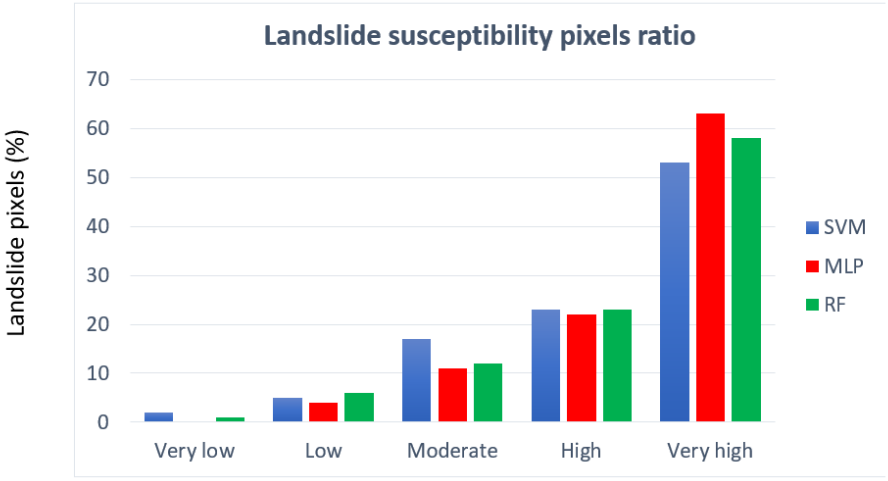

Fig.9.Landslide susceptibility pixels ratio

5. Discussion

The feature selection method is widely exploited for landslide spatial prediction to evaluate the predictive ability of landslide influencing factors to boost landslide model output by eliminating redundant or extraneous variables before learning models[60],[61]. The Pearson correlation technique was used as a function selection method in the current analysis to test the predictive capacity of landslide impacting factors to landslide models. Results of the feature selection suggest that slope demonstrated the best predictive potential for landslide models since a great deal of the identified landslide locations are on or alongside the high slope locations. There are other contributing factors in landslide models including NDVI, elevation, rainfall, aspect, the curvature of the profile, land use, TWI, the curvature of the plan, and fault distance that have also been used in other comparable inquiries [62],[63].

In landslide threat and risk evaluation, spatial prediction of landslides is believed to be among the highly challenging tasks. However, a variety of approaches have been suggested for modeling shallow landslide susceptibility. It is obvious that a landslide model's prediction accuracy relies on the exploited method. Many novel ML methods and techniques were the result of the continuing advancement of the ML sector and GIS. Thus, novel methods and techniques exploration for shallow landslide modeling are extensively essential[64],[65].

The presented problem in the study was discussed by analyzing and comparing three machine learning methods, comprising a series of highly widespread methods (e.g., the RF, the MLP Neural Nets, and the SVM). On the basis of a grid search method, SVM, MLP, and RF models were tuned to approximate the optimal structural parameters. The optimization parameter was the neurons number in the hidden layer for MLP, the cost and gamma parameters for the SVM model, and the number of trees for the RF model. Overall, in terms of total classification accuracy, the MLP Neural Nets models significantly produced superior results than the other models; nevertheless, the SVM model provides more balance with respect to PPV and NPV (Table 4,5).

The goodness-of-fit training data are suitable for four of the susceptibility models. Although it varies between the models, the MLP and SVM models display the maximum rate of fitness with AUC values of ROC being 0.931 for the MLP Neural Nets model and 0.903 for the SVM model.

However, merely AUC usage might not be the most appropriate method in the evaluation of model performance since an elevated value for the AUC in certain situations might not certify a high spatial accuracy of the models [66]. Hence, a variety of statistical assessment measures should be considered. The MLP demonstrated the maximum rate of goodness-of-fit on the basis of the model's likelihood of correct classification of pixels into the landslide class in 94.96% of the instances, which is then closely followed by the SVM model.

The findings of the analysis indicate that the implementation of GIS and ML techniques at the Landslide Zone township level is extremely reliable and applicable. Among the utilized methods for the existing problem, the MLP has appeared as the map with highest accuracy over other maps. Overall, these ML models could produce susceptibility maps for landslides with high-quality and aid to establish policies, by which it could be possible to diminish the burden of landslides [67]. Thus, to seek the fittest model in generating landslide susceptibility maps, novel ML models and state-of-the-art techniques should be opted for future modeling.

The training data of the three ML models demonstrated satisfactory goodness of fit from the methodological viewpoint. Nevertheless, with the MLP model displaying the greatest degree of fit, there are minor variations between the models. From a technical point of view, one explanation for the so-called findings could be the fact that since the MLP method demonstrates several advantages that could enhance its efficiency relative to the other two models. For instance, a) the MLP model, with its superior performance to infer meaning out of problematic or imprecise landslide occurrence patterns, which are of great complications to be construed by humans and computer algorithms; b) since ANNs belongs to nonlinear classification techniques and comprise an artificial neuron integrated group, they possess the potential to learn sophisticated interactions between variables of input and output.

In comparison, only the points along the boundary line that is labeled as the support vector, are regarded by the SVM, i.e., merely a limited amount of sampling points that would impact the classification plane and could not directly provide the probability results. Moreover, SVM demonstrates low success in the speed of training and evaluating datasets, and it is not sufficient for extremely large datasets. SVM, on the basis of statistical learning theory, possesses a solid theoretical and mathematical foundation relative to other algorithms, which allows SVM's structure and design procedure to be error-free as well as separate from users' experience [47].

In the utilization of SVM to generate LSM, there are several benefits: the SVM-based model could fittingly function with a limited group of samples; because of the kernel function, nonlinear and high-dimensional classification cases are simpler to solve through the SVM process. Nevertheless, for landslide susceptibility evaluation, there could even be overestimation problems. The SVM is consistent with the concept of structural risk minimization principle and it provides global and distinctive solutions.

Based on the obtained results, the RF demonstrated the potential to work with various forms of datasets (continuous and discrete), and datasets also do not require standardization. It could handle extensively high-dimension data. The in-between the features' interaction could be observed during the training phase. It could demonstrate the value of numerous features following the training. The pace of model training is high and the cost of computing is minimal. The RF algorithm demonstrates a decent performance and possesses a limited amount of overfitting tendency and demonstrates a decent anti-noise potential

due to the inclusion of two randomness. This method does not entail a beforehand correlation between an objective variable and the inputs and could manage data at various scales [42].

A highly significant role is taken by the designers of the neural network scheme. If they could efficiently utilize their expertise and previous knowledge in the process of network design, they might obtain further optimal network configuration. In the present analysis, after trial and error and taking the minimal mean square error into account, the optimal network design was chosen. The input neuron number is in line with the number of landslide causative factors and following an optimization phase, the neuron number in the hidden layer was calculated since it demonstrates a significant effect on the model performance [68]. Following the training phase, both the training and validation RMSE values congregate to a low-level state, which also reveals that the trained MLP demonstrates decent generalization and fitting potential. Consequently, the over-fitting problem could be considerably solved [69].

Considering that ANNs could be adapted for parallel computing platforms, the methodology could significantly take advantage of the accelerated growth of Graphics Processing Units (GPUs), in which an extensive amount of processors run training kernels parallelly, In addition, MLP has great versatility in the way that they could be trained with diverse input parameters across a variety of datasets and still have acceptable performance, with the only prerequisite being the accessible data which is adequately informative [70].

6. Conclusion and future works

To conclude, the present paper offers an assessment of the causative factors in Ahar county's landslide susceptibility evaluations and leads to a comprehensive comparison and assessment of three models of landslide susceptibility. There was a total of ten conditioning factors which were investigated. The landslide inventory database had 26 locations which were split into two groups: one for training, with 186 landslides, and another for evaluation of the model with 80 landslides. For analyzing the associations between landslides and landslide conditioning variables, the PCF model was exploited as a bivariate statistical test. Furthermore, in the present analysis, the Pearson correlation test [71] was used to measure the predictive strength of ten landslide condition variables. The Pearson technique was chosen for feature selection in machine learning because of its efficiency [72]. None of the causes is omitted in the present study since they all have predictive power for the landslide. Slope, aspect, NDVI, height, distance from fault, land usage, plan curvature, profile curvature, TWI, and rain were found to be the most powerful factors causing landslide incidence.

Three common models, MLP, RF, and SVM, were used to test and evaluate their performance on the same training and validation datasets. Comparing the performance of the MLP model reveals that it has outperformed the SVM, and RF models that were utilized as benchmark methods. In general, relative to the other models, the Neural Network based model had a more robust classification efficiency. The MLP model, despite its excellent efficiency, is primarily affected by the structural parameters tuning processes.

Based on the optioned results, our future work will focus on applying the optimized ML methods for landslide mapping, part of our future work will also take place to apply the integrated approach of deep learning methods and object-based image analysis methods for semi/automate landslide detecting and delineation from earth observation satellite image. In conclusion, the extracted map from the MLP Neural Nets method is ideally adapted with the aim of aiding land use planning and landslide

alleviation. The urbanization progress in this area would raise the burden on both the economy and population, demonstrates the utmost relevance the of present study's findings. It is anticipated that the produced landslide susceptibility map would be beneficial for urban planners and government officials in planning the region's development.

Acknowledgments The authors thank the Iranian Department of Water Resources Management (IDWRM), Iranian Statistical Institute (ISI), and Meteorological Organization (MetO) for providing whole investigation reports. We are grateful to all those who helped us for their expert comments.

Conflict of interest The authors declare that they have no conflict of interest.

References

[1] J. Zêzere, S. Pereira, R. Melo, S. Oliveira, and R. A. Garcia, "Mapping landslide susceptibility using data-driven methods," Science of the total environment, vol. 589, pp. 250-267, 2017.

[2] L. Saro, J. S. Woo, O. Kwan-Young, and L. Moung-Jin, "The spatial prediction of landslide susceptibility applying artificial neural network and logistic regression models: A case study of Inje, Korea," Open Geosciences, vol. 8, no. 1, pp. 117-132, 2016.

[3] B. Feizizadeh and T. Blaschke, "An uncertainty and sensitivity analysis approach for GIS-based multicriteria landslide susceptibility mapping," International Journal of Geographical Information Science, vol. 28, no. 3, pp. 610-638, 2014.

[4] H. Hong et al., "Landslide susceptibility assessment at the Wuning area, China: A comparison between multi-criteria decision making, bivariate statistical and machine learning methods," Natural Hazards, vol. 96, no. 1, pp. 173-212, 2019.

[5] Q. Wang, Y. Guo, W. Li, J. He, and Z. Wu, "Predictive modeling of landslide hazards in Wen County, northwestern China based on information value, weights-of-evidence, and certainty factor," Geomatics, Natural Hazards and Risk, vol. 10, no. 1, pp. 820-835, 2019.

[6] D. D. Kose and T. Turk, "GIS-based fully automatic landslide susceptibility analysis by weight-of-evidence and frequency ratio methods," Physical Geography, vol. 40, no. 5, pp. 481-501, 2019.

[7] Y. Li and W. Chen, "Landslide susceptibility evaluation using hybrid integration of evidential belief function and machine learning techniques," Water, vol. 12, no. 1, p. 113, 2020.

[8] S. Mondal and S. Mandal, "Landslide susceptibility mapping of Darjeeling Himalaya, India using index of entropy (IOE) model," Applied Geomatics, vol. 11, no. 2, pp. 129-146, 2019.

[9] R. Costache, H. Hong, and Y. Wang, "Identification of torrential valleys using GIS and a novel hybrid integration of artificial intelligence, machine learning and bivariate statistics," Catena, vol. 183, p. 104179, 2019.

[10] A. M. Youssef, H. R. Pourghasemi, Z. S. Pourtaghi, and M. M. Al-Katheeri, "Landslide susceptibility mapping using random forest, boosted regression tree, classification and regression tree, and general linear models and comparison of their performance at Wadi Tayyah Basin, Asir Region, Saudi Arabia," Landslides, vol. 13, no. 5, pp. 839-856, 2016.

[11] F. Falah and H. Zeinivand, "Gis-based groundwater potential mapping in khorramabad in lorestan, Iran, using frequency ratio (fr) and weights of evidence (woe) models," Water Resources, vol. 46, no. 5, pp. 679-692, 2019.

[12] I. C. Nicu, "Application of analytic hierarchy process, frequency ratio, and statistical index to landslide susceptibility: an approach to endangered cultural heritage," Environmental earth sciences, vol. 77, no. 3, p. 79, 2018.

[13] S. Lee, M.-J. Lee, H.-S. Jung, and S. Lee, "Landslide susceptibility mapping using naïve bayes and bayesian network models in Umyeonsan, Korea," Geocarto international, vol. 35, no. 15, pp. 1665-1679, 2020.

[14] P. Tsangaratos and I. Ilia, "Comparison of a logistic regression and Naïve Bayes classifier in landslide susceptibility assessments: The influence of models complexity and training dataset size," Catena, vol. 145, pp. 164-179, 2016.

[15] H. Ebrahimy, B. Feizizadeh, S. Salmani, and H. Azadi, "A comparative study of land subsidence susceptibility mapping of Tasuj plane, Iran, using boosted regression tree, random forest and classification and regression tree methods," Environmental Earth Sciences, vol. 79, pp. 1-12, 2020.

[16] A. A. Shahri, J. Spross, F. Johansson, and S. Larsson, "Landslide susceptibility hazard map in southwest Sweden using artificial neural network," Catena, vol. 183, p. 104225, 2019.

[17] S.-J. Park, C.-W. Lee, S. Lee, and M.-J. Lee, "Landslide susceptibility mapping and comparison using decision tree models: A Case Study of Jumunjin Area, Korea," Remote Sensing, vol. 10, no. 10, p. 1545, 2018.

[18] H. A. Gheshlaghi and B. Feizizadeh, "An integrated approach of analytical network process and fuzzy based spatial decision making systems applied to landslide risk mapping," Journal of African Earth Sciences, vol. 133, pp. 15-24, 2017.
[19] A.-X. Zhu et al., "A similarity-based approach to sampling absence data for landslide susceptibility mapping using data-driven methods," Catena, vol. 183, p. 104188, 2019.
[20] Z. Fang, Y. Wang, L. Peng, and H. Hong, "Integration of convolutional neural network and conventional machine learning classifiers for landslide susceptibility mapping," Computers & Geosciences, vol. 139, p. 104470, 2020.
[21] T. V. Phong et al., "Landslide susceptibility modeling using different artificial intelligence methods: A case study at Muong Lay district, Vietnam," Geocarto International, pp. 1-24, 2019.
[22] Y. Tian, L. A. Owen, C. Xu, L. Shen, Q. Zhou, and P. M. Figueiredo, "Geomorphometry and statistical analyses of landslides triggered by the 2015 Mw 7.8 Gorkha earthquake and the Mw 7.3 aftershock, Nepal," Frontiers in Earth Science, vol. 8, p. 407, 2020.
[23] K. Mohammadzadeh and B. Feizizadeh, "Identifying and Monitoring Soil Salinization in the Eastern Part of Urmia lake Together With Comparing Capability of Object Based Image Analysis Techniques," Journal of Water and Soil Conservation, vol. 27, no. 3, pp. 65-84, 2020.
[24] B. Shokati and B. Feizizadeh, "Sensitivity and uncertainty analysis of agro-ecological modeling for saffron plant cultivation using GIS spatial decision-making methods," Journal of Environmental Planning and Management, vol. 62, no. 3, pp. 517-533, 2019.
[25] B. Feizizadeh, H. A. Gheshlaghi, and D. T. Bui, "An integrated approach of GIS and hybrid intelligence techniques applied for flood risk modeling," Journal of Environmental Planning and Management, pp. 1-32, 2020.
[26] B. Feizizadeh, M. K. Garajeh, T. Blaschke, and T. Lakes, "An object based image analysis applied for volcanic and glacial landforms mapping in Sahand Mountain, Iran," Catena, vol. 198, p. 105073, 2021.
[27] H. Abedi Gheshlaghi, B. Feizizadeh, and T. Blaschke, "GIS-based forest fire risk mapping using the analytical network process and fuzzy logic," Journal of Environmental Planning and Management, vol. 63, no. 3, pp. 481-499, 2020.
[28] B. Feizizadeh, T. Blaschke, and H. Nazmfar, "GIS-based ordered weighted averaging and Dempster–Shafer methods for landslide susceptibility mapping in the Urmia Lake Basin, Iran," International Journal of Digital Earth, vol. 7, no. 8, pp. 688-708, 2014.
[29] O. Ghorbanzadeh, S. Pourmoradian, T. Blaschke, and B. Feizizadeh, "Mapping potential nature-based tourism areas by applying GIS-decision making systems in East Azerbaijan Province, Iran," Journal of Ecotourism, vol. 18, no. 3, pp. 261-283, 2019.
[30] B. Feizizadeh and T. Blaschke, "GIS-multicriteria decision analysis for landslide susceptibility mapping: comparing three methods for the Urmia lake basin, Iran," Natural hazards, vol. 65, no. 3, pp. 2105-2128, 2013.
[31] B. Feizizadeh, M. S. Roodposhti, P. Jankowski, and T. Blaschke, "A GIS-based extended fuzzy multi-criteria evaluation for landslide susceptibility mapping," Computers & geosciences, vol. 73, pp. 208-221, 2014.
[32] S. Lee, J. Hwang, and I. Park, "Application of data-driven evidential belief functions to landslide susceptibility mapping in Jinbu, Korea," Catena, vol. 100, pp. 15-30, 2013.
[33] H. Hong, H. R. Pourghasemi, and Z. S. Pourtaghi, "Landslide susceptibility assessment in Lianhua County (China): a comparison between a random forest data mining technique and bivariate and multivariate statistical models," Geomorphology, vol. 259, pp. 105-118, 2016.
[34] W. Chen, H. R. Pourghasemi, and S. A. Naghibi, "A comparative study of landslide susceptibility maps produced using support vector machine with different kernel functions and entropy data mining models in China," Bulletin of Engineering Geology and the Environment, vol. 77, no. 2, pp. 647-664, 2018.
[35] B. T. Pham, D. T. Bui, M. Dholakia, I. Prakash, and H. V. Pham, "A comparative study of least square support vector machines and multiclass alternating decision trees for spatial prediction of rainfall-induced landslides in a tropical cyclones area," Geotechnical and Geological Engineering, vol. 34, no. 6, pp. 1807-1824, 2016.
[36] H. Hong, W. Chen, C. Xu, A. M. Youssef, B. Pradhan, and D. Tien Bui, "Rainfall-induced landslide susceptibility assessment at the Chongren area (China) using frequency ratio, certainty factor, and index of entropy," Geocarto international, vol. 32, no. 2, pp. 139-154, 2017.
[37] W. Chen et al., "A comparative study of logistic model tree, random forest, and classification and regression tree models for spatial prediction of landslide susceptibility," Catena, vol. 151, pp. 147-160, 2017.
[38] D. Tien Bui, B. T. Pham, Q. P. Nguyen, and N.-D. Hoang, "Spatial prediction of rainfall-induced shallow landslides using hybrid integration approach of Least-Squares Support Vector Machines and differential evolution optimization: a case study in Central Vietnam,"

International Journal of Digital Earth, vol. 9, no. 11, pp. 1077-1097, 2016.
[39] C. Zhao, W. Chen, Q. Wang, Y. Wu, and B. Yang, "A comparative study of statistical index and certainty factor models in landslide susceptibility mapping: a case study for the Shangzhou District, Shaanxi Province, China," Arabian Journal of Geosciences, vol. 8, no. 11, pp. 9079-9088, 2015.
[40] H. R. Pourghasemi and O. Rahmati, "Prediction of the landslide susceptibility: which algorithm, which precision?," Catena, vol. 162, pp. 177-192, 2018.
[41] V. K. Pandey, K. K. Sharma, H. R. Pourghasemi, and S. K. Bandooni, "Sedimentological characteristics and application of machine learning techniques for landslide susceptibility modelling along the highway corridor Nahan to Rajgarh (Himachal Pradesh), India," Catena, vol. 182, p. 104150, 2019.
[42] Z. Fang, Y. Wang, L. Peng, and H. Hong, "Integration of convolutional neural network and conventional machine learning classifiers for landslide susceptibility mapping," Computers & Geosciences, p. 104470, 2020.
[43] M. Elmoulat, O. Debauche, S. Mahmoudi, S. A. Mahmoudi, P. Manneback, and F. Lebeau, "Edge computing and artificial intelligence for landslides monitoring," Procedia Computer Science, vol. 177, pp. 480-487, 2020.
[44] N. Kausar and A. Majid, "Random forest-based scheme using feature and decision levels information for multi-focus image fusion," Pattern Analysis and Applications, vol. 19, no. 1, pp. 221-236, 2016.
[45] J. Dou et al., "Evaluating GIS-based multiple statistical models and data mining for earthquake and rainfall-induced landslide susceptibility using the LiDAR DEM," Remote Sensing, vol. 11, no. 6, p. 638, 2019.
[46] J. Dou et al., "Optimization of causative factors for landslide susceptibility evaluation using remote sensing and GIS data in parts of Niigata, Japan," PloS one, vol. 10, no. 7, p. e0133262, 2015.
[47] V.-H. Nhu et al., "Shallow Landslide Susceptibility Mapping: A Comparison between Logistic Model Tree, Logistic Regression, Naïve Bayes Tree, Artificial Neural Network, and Support Vector Machine Algorithms," International Journal of Environmental Research and Public Health, vol. 17, no. 8, p. 2749, 2020.
[48] D. T. Bui, P. Tsangaratos, V.-T. Nguyen, N. Van Liem, and P. T. Trinh, "Comparing the prediction performance of a Deep Learning Neural Network model with conventional machine learning models in landslide susceptibility assessment," Catena, vol. 188, p. 104426, 2020.
[49] M. Alizadeh et al., "Social vulnerability assessment using artificial neural network (ANN) model for earthquake hazard in Tabriz city, Iran," Sustainability, vol. 10, no. 10, p. 3376, 2018.
[50] A. M. S. Pradhan and Y.-T. Kim, "Spatial data analysis and application of evidential belief functions to shallow landslide susceptibility mapping at Mt. Umyeon, Seoul, Korea," Bulletin of Engineering Geology and the Environment, vol. 76, no. 4, pp. 1263-1279, 2017.
[51] W. Chen, X. Xie, J. Peng, J. Wang, Z. Duan, and H. Hong, "GIS-based landslide susceptibility modelling: a comparative assessment of kernel logistic regression, Naïve-Bayes tree, and alternating decision tree models," Geomatics, Natural Hazards and Risk, vol. 8, no. 2, pp. 950-973, 2017.
[52] E. K. Yesilnacar, The application of computational intelligence to landslide susceptibility mapping in Turkey. University of Melbourne, Department, 200., 2005.
[53] W. Chen et al., "GIS-based landslide susceptibility evaluation using a novel hybrid integration approach of bivariate statistical based random forest method," Catena, vol. 164, pp. 135-149, 2018.
[54] T. Ngo, "Data mining: practical machine learning tools and technique, by ian h. witten, eibe frank, mark a. hell," ACM SIGSOFT Software Engineering Notes, vol. 36, no. 5, pp. 51-52, 2011.
[55] P. R. Kadavi, C.-W. Lee, and S. Lee, "Application of ensemble-based machine learning models to landslide susceptibility mapping," Remote Sensing, vol. 10, no. 8, p. 1252, 2018.
[56] T. Kavzoglu, E. K. Sahin, and I. Colkesen, "Selecting optimal conditioning factors in shallow translational landslide susceptibility mapping using genetic algorithm," Engineering Geology, vol. 192, pp. 101-112, 2015.
[57] K. Martinović, K. Gavin, and C. Reale, "Development of a landslide susceptibility assessment for a rail network," Engineering Geology, vol. 215, pp. 1-9, 2016.
[58] B. Pradhan and S. Lee, "Delineation of landslide hazard areas on Penang Island, Malaysia, by using frequency ratio, logistic regression, and artificial neural network models," Environmental Earth Sciences, vol. 60, no. 5, pp. 1037-1054, 2010.
[59] B. Pradhan and S. Lee, "Regional landslide susceptibility analysis using back-propagation neural network model at Cameron Highland,

Malaysia," Landslides, vol. 7, no. 1, pp. 13-30, 2010.
[60] W. Chen et al., "Spatial prediction of landslide susceptibility using gis-based data mining techniques of anfis with whale optimization algorithm (woa) and grey wolf optimizer (gwo)," Applied Sciences, vol. 9, no. 18, p. 3755, 2019.
[61] B. T. Pham et al., "A novel hybrid approach of landslide susceptibility modelling using rotation forest ensemble and different base classifiers," Geocarto International, vol. 35, no. 12, pp. 1267-1292, 2020.
[62] M. Bayat, M. Ghorbanpour, R. Zare, A. Jaafari, and B. T. Pham, "Application of artificial neural networks for predicting tree survival and mortality in the Hyrcanian forest of Iran," Computers and Electronics in Agriculture, vol. 164, p. 104929, 2019.
[63] D. Van Dao et al., "A spatially explicit deep learning neural network model for the prediction of landslide susceptibility," Catena, vol. 188, p. 104451, 2020.
[64] Y. Wang, Z. Fang, H. Hong, and L. Peng, "Flood susceptibility mapping using convolutional neural network frameworks," Journal of Hydrology, vol. 582, p. 124482, 2020.
[65] Y. Wang, Z. Fang, M. Wang, L. Peng, and H. Hong, "Comparative study of landslide susceptibility mapping with different recurrent neural networks," Computers & Geosciences, vol. 138, p. 104445, 2020.
[66] O. Ghorbanzadeh, T. Blaschke, K. Gholamnia, S. R. Meena, D. Tiede, and J. Aryal, "Evaluation of different machine learning methods and deep-learning convolutional neural networks for landslide detection," Remote Sensing, vol. 11, no. 2, p. 196, 2019.
[67] Q. He et al., "Landslide spatial modelling using novel bivariate statistical based Naïve Bayes, RBF Classifier, and RBF Network machine learning algorithms," Science of the total environment, vol. 663, pp. 1-15, 2019.
[68] D. Tien Bui et al., "A novel integrated approach of relevance vector machine optimized by imperialist competitive algorithm for spatial modeling of shallow landslides," Remote Sensing, vol. 10, no. 10, p. 1538, 2018.
[69] C. Polykretis and C. Chalkias, "Comparison and evaluation of landslide susceptibility maps obtained from weight of evidence, logistic regression, and artificial neural network models," Natural hazards, vol. 93, no. 1, pp. 249-274, 2018.
[70] S. P. Panda, "Enhancing the Proficiency of Artificial Neural Network on Prediction with GPU," in 2019 International Conference on Machine Learning, Big Data, Cloud and Parallel Computing (COMITCon), 2019, pp. 67-71: IEEE.
[71] A. Shirzadi et al., "Shallow landslide susceptibility assessment using a novel hybrid intelligence approach," Environmental Earth Sciences, vol. 76, no. 2, p. 60, 2017.
[72] P. Reichenbach, M. Rossi, B. D. Malamud, M. Mihir, and F. Guzzetti, "A review of statistically-based landslide susceptibility models," Earth-Science Reviews, vol. 180, pp. 60-91, 2018.